HHS Public Access

Author manuscript

Cryobiology. Author manuscript; available in PMC 2020 September 02.

Published in final edited form as:

Cryobiology. 2018 June ; 82: 106–111. doi:10.1016/j.cryobiol.2018.03.012.

Pirfenidone inhibits cryoablation induced local macrophage infiltration along with its associated TGFb1 expression and serum cytokine level in a mouse model

Yangkui Gu, M.D., Ph.D.[1,2], **Govindarajan Srimathveeravalli, Ph.D.**[1], **Liqun Cai, M.B.**[1], **Eisuke Ueshima, M.D., Ph.D.**[1], **Majid Maybody, M.D.**[1], **Hooman Yarmohammadi, M.D.**[1], **Yuan-Shan Zhu, M.D., Ph.D.**[3], **Jeremy C Durack, M.D.**[1], **Stephen B Solomon, M.D.**[1], **Jonathan A Coleman, M.D.**[1], **Joseph P Erinjeri, M.D., Ph.D.**[1,*]

[1]Department of Radiology, Memorial Sloan Kettering Cancer Center, 1275 York Avenue, H-118, New York, NY 10065, USA

[2]Microinvasive Interventional Department, Sun Yat-sen University Cancer Center, Guangzhou, Guangdong, 510060, P. R. China

[3]Clinical and Translational Science Center, Weill Cornell Medicine, New York, NY 10065, USA

Abstract

Purpose: To investigate the effects of pirfenidone (PFD) on post-cryoablation inflammation in a mouse model.

Materials and methods: In this IACUC-approved study, eighty Balb/c mice were randomly divided into four groups (20/group): sham+vehicle, sham+PFD, cryoablation+vehicle, and cryoablation+PFD. For cryoablation groups, a 20% freeze rate cryoablation (20 seconds to less than −100°C) was used to ablate normal muscle in the right flank. For sham groups, the cryoprobe was advanced into the flank and maintained for 20 seconds without ablation. PFD or vehicle solution was intraperitoneally injected (5 mg/kg) at days 0, 1, 2, 3, and then every other day until day 13 after cryoablation. Mice were euthanized at days 1, 3, 7, and 14. Blood samples were used for serum IL-6, IL-10, and TGFβ1 analysis using electrochemiluminescence and ELISA assays, respectively. Immunohistochemistry-stained ablated tissues were used to analyze macrophage infiltration and local TGFβ1 expression in the border region surrounding the cryoablation-induced coagulation zone.

Results: Cryoablation induced macrophage infiltration and increased TGFβ1 expression in the border of the necrotic zone, and high levels of serum IL-6, peaking at days 7 (70.5±8.46/HPF), 14 (228±18.36/HPF), and 7 (298.67±92.63), respectively. Animals receiving PFD showed reduced macrophage infiltration (35.5±16.93/HPF at day 7, $p<0.01$) and cytokine levels (60.2±7.6/HPF at

Corresponding Author: Joseph P Erinjeri, M.D., Ph.D., Department of Radiology, Memorial Sloan Kettering Cancer Center, 1275 York Avenue, H-118, New York, NY 10065, USA; erinjerj@mskcc.org.

Conflict of Interest Notification: There are no any actual or potential conflicts of interest exist.

day 14, p<0.01). PFD also significantly reduced serum IL-6 levels (p<0.001 vs. all non-PFD groups).

Conclusions: PFD mitigates cryoablation induced muscle tissue macrophage infiltration, increased IL-6 levels, and local TGFβ1 expression in a small animal model.

Keywords

cryoablation; macrophage; IL-6; TGFβ1; pirfenidone

Introduction

Cryoablation is a minimally invasive technique used to treat various malignant neoplasms, including malignancies of the skin, prostate, liver, lung, bone, and the breast [20]. Tissue injury is induced by mechanical disruption of cell membranes and vascular stasis. Following tissue injury, local inflammation surrounds the area of tissue necrosis.

Gazzaniga et al demonstrated the inflammatory changes that take place after cryosurgery-induced necrosis in a human melanoma xenograft model using nude mice [9]. Neutrophils appeared during the early stage of inflammation, while macrophages became more abundant at day 3 and peaked at day 7. Stromal peritumoral fibroblasts showed increasing size and number from days 7 to 15.

Macrophages are an important part of the post-treatment wound healing response following ablation. They secrete cytokines such as tissue hepatocyte growth factor (HGF) that help to heal the tissue. However, they can also have an off-target effect on residual tumor cells, bestowing survival benefit to residual cancer cells in the treatment region [19]. In addition, several secreted cytokines such as IL-6 and TGFβ1 may stimulate cancer regeneration and survival after thermoablation. Erinjeri et al [6] reported increased plasma levels of IL-6 and IL-10 after thermoablation especially in the case of cryoablation. While TGFβ1 is considered a central mediator of injury repair and fibrosis, inducing extracellular matrix production and proliferation of myofibroblasts and fibroblasts. TGFβ1 also induces epithelial-mesenchymal transition, promotion of angiogenesis and cancer cell invasion [8], and suppression of the immune system at the later stages of cancer progression [4]. Thus, its increased presence may elevate the potential for tumor recurrence and metastasis [32].

Pirfenidone [5-methyl-1-phenyl-2-(1H)-pyridone, PFD] is an anti-fibrotic and anti-inflammatory agent approved for idiopathic fibrosis of the lung. The aim of this study is to investigate the effects of pirfenidone on post-cryoablation inflammation in a normal small animal model. We hypothesize that cryoablation will lead to macrophage infiltration and increased TGFβ1 expression at the ablated border. Pirfenidone will attenuate or even block this local environment change and change macrophage-related serum cytokine levels.

Materials and Methods

Animals

Experiments were conducted with approval from the institutional animal care and use committee (IACUC). Eighty female Balb/c mice 10–12 weeks old (Jackson Laboratory, Bar Harbor, ME) were bred, housed and treated according to approved institutional animal protocols. All animals were maintained on a 12-hour light-dark cycle in a specific pathogen-free animal facility with free access to food and water.

Treatment and control groups

Two weeks before cryoablation, retro orbital blood collection was performed in 6 randomly selected mice to test for serum cytokines baseline level. Then these 6 mice were mixed with the remaining 74 mice. All 80 mice were randomly divided into 4 groups (20/each group): 1) sham + vehicle, 2) sham + PFD, 3) cryoablation (CA) +vehicle, and 4) cryoablation (CA) + PFD.

Preparation of pirfenidone and vehicle solutions

To prepare the pirfenidone solution, 500 mg pirfenidone (Selleckchem, Munich, Germany) was dissolved in 1.0 ml dimethyl sulfoxide (DMSO) (Gaylord Chemical, USA). The resulting solution was sonicated in a water bath at about 45 °C until transparent. Then 15 ml polyethylene glycol (PEG)-300 (Med Lab Supply, Miami, USA) was added. The mixture was diluted with double distilled water DDH_2O to 100 ml (5 mg/ml). The intraperitoneal injection dose was 50 mg/kg. The vehicle injection was prepared as above minus pirfenidone, resulting in a DMSO+PEG-300+DDH_2O mixed solution. The detailed injection protocol is presented in Fig. 1.

Cryoablation protocol

Isoflurane inhalation anesthesia and carprofen were administered before cryoablation. The mice were surgically prepped by shaving the right flank. They were washed with alternating ovidone-iodine scrub and 70% alcohol rinse. A small cut in the skin enabled introduction of the cryoprobe (Endocare 1.7mm PerCryo) into the skeletal muscle of the right flank in animals. The depth of puncture was 5 mm. Freezing was administered for 20 seconds to less than −100°C at the needle hub at 20% freeze rate. For the two sham groups, we advanced the cryoprobe into the flank where it was maintained for 20 seconds without ablation. After ablation, the site was monitored for bleeding or any other post procedural complications. If needed, carprofen was administrated every 12 hours for pain relief during the first 3 days post ablation.

Blood and tissue sample collection

After cryoablation, blood samples were drawn from a retro orbital vein from anesthetized mice before they were euthanized. After clotting and centrifugation, sera were fractionated and stored at −80°C. Mice were euthanized at day 1, day 3, day 7, and day 14 (prescribed study endpoints). Ablated tissues were harvested and fixed in 10% neutral buffered formalin. They were sectioned at 4–7 μm and stained with immunohistochemistry (IHC) (Fig.1).

IHC

F4/80 for macrophage—The IHC detection of F4/80 Ab was performed by the Molecular Cytology Core Facility of Memorial Sloan Kettering Cancer Center using the Discovery XT processor (Ventana Medical Systems, Oro Valley, AZ). A rat F4/80 antibody (Abcam, Cambridge, UK, cat #ab6640) was used at 2 ug/ml concentrations. The protocol involved blocking (10% normal rabbit serum, 2% bovine serum albumin (BSA)) for 30 min, 3-hour incubation with primary antibody, followed by 60-min incubation with biotinylated rabbit anti-rat IgG (Vector Laboratories, Burlingame, CA, cat #BA-4000, 1:200 dilution). Blocker D, Streptavidin- HRP, and DAB detection kits (Ventana Medical Systems, Oro Valley, AZ) were used according to the manufacturer's instructions.

TGFβ1 Staining

Paraffin sections were dewaxed in xylene and hydrated into graded alcohols. Endogenous peroxidase activity was blocked by immersing the slides in 1% hydrogen peroxide in phosphate-buffered saline (PBS) for 15 minutes. Pretreatment was performed in a steamer using 10 mM citrate buffer, pH 6.0, for 30 minutes. Sections were incubated overnight with the primary antibody, anti-TGFβ1 antibody (Rabbit polyclonal from Abcam, Cambridge, UK, cat. #ab92486) diluted 1:50. Sections were washed with PBS and incubated with the appropriate secondary antibody followed by avidin-biotin complexes (Vector Laboratories, Burlingame, CA, cat. #PK-6100). Antibody reactions were visualized with 3–3' diaminobenzidine (Sigma-Aldrich, St. Louis, MO, cat. #D8001) and counterstained with hematoxylin. Tissue sections were dehydrated in graded alcohols, cleared in xylene, and mounted.

Count of F4/80and TGFβ1 positive cells were evaluated with the Image J software [23].

Cytokines

Serum levels of IL-6 and IL-10 were measured using the mouse V-PLEX Proinflammatory Panel 1 mouse kit (Meso Scale Discovery, Rockville, MD, Cat. #K0080001) using an electrochemiluminescence detection technology following the manufacturer's instruction. Serum levels of TGFβ1 were determined using the Mouse/Rat/Porcine/Canine TGF-beta 1 Quantikine ELISA Kit (R&D Systems, Minneapolis, MN, Cat. #MB100B) according to the manufacturer's instruction.

Statistical analysis

All quantitative data were presented as mean ± SD. The ANOVA was used to determine statistical significance. The significance level (α) on all statistical analysis was predefined at 0.05.

Results

Cryoablation induced macrophage infiltration and TGFβ1 expression

Compared with the sham groups, the CA groups demonstrated increased infiltration of F4/80 positive cells from day 3 to day 14 (Table 1) and TGFβ1 expression from day 1 to day 14 (Table 2), as determined by IHC staining of the geographic rim surrounding the treatment

zone. There was a significant difference between the CA groups and the sham groups ($p<0.001$). The number of macrophages peaked at day 7 following cryoablation (Fig 2a, Fig 2b) and TGFβ1 expression peaked at day 14 (Fig 3a, Fig 3b).

Pirfenidone reduces infiltration of macrophages into region of cryoablation

When comparing both CA groups, the CA + vehicle group had higher macrophage infiltration in normal muscle at day 7 and day 14 compared with the CA + PFD group (Table 1). There was a significant difference between the two groups for the count of F4/80 positive cells at day7 (70.5±8.46/high-power field (HPF) vs 35.5±16.93/HPF, $p=0.001$) and day 14 (55.5±9.07/HPF vs 18.2±3.66/HPF, $p<0.001$) (Fig 2a, 2b).

Pirfenidone reduces local expression of TGFβ1 in region of cryoablation

When comparing both CA groups, the CA + vehicle group had higher local TGFβ1 expression in normal muscle (Table 2) at day 7 and day 14 compared with the CA + PFD group. There was a significant difference between the two groups for the count of the TGFβ1 expression positive cells at day 7 (183±9.59/HPF vs 60.2±7.6/HPF, $p<0.001$) and day 14 (228±18.36/HPF vs 65.6±8.73/HPF, $p<0.001$) (Fig 3a, 3b).

Pirfenidone reduces systemic levels of IL-6 following cryoablation

Compared with baseline level cytokine levels, all groups had a transient elevation of serum IL-6 at day 1 due to puncture or CA damage (Table 3). IL-6 levels peaked on day 7 for the CA + vehicle group, showing a significant rise from 7.33 at baseline to 298.67 pg/ml ($p<0.001$). IL-6 levels for the CA + vehicle group were significantly higher compared with the CA + PFD group at day 7 (16.28 vs 298.67 pg/ml, $p<0.001$) as well as at day 14 (7.78 vs 121.33 pg/ml, $p<0.001$) (Fig 4). IL-10 and TGFβ1 showed no significant changes in serum levels at day 14 of cryoablation in all groups.

Discussion

Cryoablation is a commonly used method for treating a variety of cancers with benefits with respect to surgery. As a minimally invasive, image-guidable, and repeatable procedure, it is generally associated with improved patient comfort, lower complication risk, and reduced cost. Compared with surgery, another potential benefit of cryoablation is the ability to freeze tumors and a margin of adjacent normal tissue, which remain in situ with the potential to stimulate an immunologic response.

Three days after cryoablation, five histological zones extending radially outward from the cryoablation probe can be found, including central necrosis, inflammation, thrombosis/ischemic necrosis, granulation, and viable tumor [15]. Viable tumor is not always observed after cryoablation if the procedure is completely effective. These zones are time-dependent not only for cryoablation but also following heat-based modalities such as radiofrequency ablation [15, 19]. In the present study, F4/80 immunohistochemistry staining revealed that macrophages began to accumulate at the border zone starting at day 3 and peaking at day 7 and then decreased gradually. Local TGFβ1 expression enhanced gradually from day 1 to day 14 and its peak occurred at day 14, the latest endpoint in this study. Our results are

consistent with published studies [9, 15, 19] showing that peri-ablation infiltration zones changes are also time-dependent. We observed a monotonous rise in TGFβ1 expression till day 14 after cryoablation in the group of mice receiving cryoablation without post-treatment PFD, but as that was the endpoint of our study, we do not know whether local TGFβ1 expression will continue to rise after this timepoint. We were able to determine that peak time differs from time to peak macrophages infiltration. Our observations suggest that there must be other sources of local TGFβ1 expression.

Macrophages, as vital immune cells, play an important role in immunomodulation after cryoablation. They not only clean necrotic cells but also secrete various cytokines that will activate other immune related cells such as IL-6, a key secreted cytokine. In non-infectious inflammations, such as cryoablation injury, damage-associated molecular patterns (DAMPs) from damaged or dying cells stimulate toll-like receptors of macrophages to produce IL-6 [18]. In our study, both the number of local infiltrated macrophages and serum IL-6 levels peaked at day 7 and decreased at day 14 after cryoablation. With intraperitoneal PFD injection, however, they decreased conformably, compared with CA alone group. This shows that post-ablation serum IL-6 is mainly secreted by local infiltrated macrophages.

Our study found that PFD can decrease post-cryoablation induced macrophages infiltration and serum IL-6 levels, with several potential ramifications for tumor cryoablation. IL-6 is reported to help liver recovery after injury by activating the NF-kB (Nuclear Factor Kappa-light-chain-enhancer of activated B cells) and STAT3 (Signal Transducer and Activator of Transcription 3) signaling pathways [5]. IL-6 also supports cancer cell survival and promotes the growth of lung, colon, liver cancers [11–13, 31]. Many studies have revealed that patients with high plasma levels of IL-6 had shorter hepatocellular carcinoma-free survival than those with low IL-6 levels [14, 30]. After incomplete cryoablation, viable or sub-lethal tumor cells that persist in the margin may be stimulated to proliferate by elevated serum IL-6. Thus, IL-6 is an attractive potential target in decreasing the rate of local recurrence and/or distant metastasis after cryoablation. Decreasing the secretion level of IL-6 or affecting its downstream targets can be a useful combined therapy. To limit increased IL-6 levels, decreasing macrophage infiltration may be a good strategy. Cryoablation or other thermoablation modality plus PFD may prove very useful for future research and eventual clinical translation.

TGFβ1 is a frequently studied cytokine in the fields of cancer, auto-immune disease, and infectious disease. TGFβ1 causes immune suppression and angiogenesis, which makes the cancer more invasive [1]. One of the pivotal mechanisms of active immune suppression is mediated by cytokine TGFβ1 or CD4+Foxp3+Tregcells [17, 22]. Interleukin-1 and interleukin 2 dependent proliferation of activated T cells [26, 28], and the activation of quiescent helper T cells and cytotoxic T cells are prevented by the activation of TGFβ1 [10, 29]. Thus, local excessive TGFβ1 expression is a negative factor in tumor microenvironment. Our results reveal that cryoablation can induce high expression of TGFβ1 at the local peri-ablation zone and PFD can attenuate TGFβ1 expression after cryoablation, which may have benefits for promotion of local immune status around ablated tumor, especially for killing the sub-lethal survival cancer cells. Although local TGFβ1 expression increased gradually in 14 days in the cryoablation groups, there is no significant

elevation in serum TGFβ1 level compared with the sham groups. This shows that local serum cytokine levels could vary greatly from those in plasma.

Cells of monocytic lineage, such as macrophages and dendritic cells, play an important role in mediating post-cryoablation immunologic response, with implications for abscopal control of distant tumors. While not conclusive, Sable et al. [20] report that macrophages infiltrating cryoablation typically suppress the immunologic response, while dendritic cells promote priming of the adaptive immune system through cross presentation of antigens from the region of cryoablation. The suppressive action of macrophages could be largely derived from IL-6 and TGFβ1 secretion, and our results demonstrate that such effects can be overcome with adjuvant administration of PFD. The specific impact of PFD on treatment on dendritic cells, and priming of the immune system was not studied as part of our work, however, we hypothesize that cryoablation with adjuvant PFD should augment cancer control.

PFD is an anti-fibrotic drug for the treatment of idiopathic pulmonary fibrosis, via the regulation of TGF-b and procollagen I and II production [16, 25, 27]. Most studies involving PFD focus on its anti-fibrotic effect [2, 3, 24]. Therefore, we were interested in whether PFD has any active effect on cryoablation induced local and systemic immunomodulation according to its pharmaceutic principal. Our data indicate that PFD can also reduce cryoablation induced macrophage infiltration, IL-6 secretion, and local TGFβ1 expression.

This study has several limitations. Firstly, it was a preliminary study and the cryoablation protocol was performed in normal muscle tissue in a small animal model. Results from a tumor xenograft animal model would be more reliable. In the future we will use a tumor xenograft animal model to repeat this study. Secondly, we tested only one cryoablation parameter. Different ablation modes may have different immunomodulation effects. Sabel et al reported that the high freeze rate of cryoablation led to fewer lung metastases and longer survival in a breast cancer mice model [21]. Thus, future studies should be performed to validate these results with different parameters. Finally, we did not test different PFD injection protocol and dosage, and its latent toxicity. PFD can increase hepatic enzyme levels, especially those of aspartate transaminase (AST), alaninetransaminase (ALT), and gamma-glutamyltranspeptidase (GGT) and is contraindicated in patients who have severe hepatic impairment [7].

In conclusion, cryoablation can induce macrophage infiltration, high serum IL-6 levels, and local TGFβ1 expression in normal muscle tissue in a small animal model. PFD can attenuate these changes.

Acknowledgments

Funding: This research was supported in part through the NIH/NCI Cancer Center Support Grant P30 CA008748, and NIH/NCATS grant UL1 TR000457. The funding source had no involvement in the study design; in the collection, analysis and interpretation of data; in the writing of the report; and in the decision to submit the article for publication.

Abbreviations:

BSA	bovine serum albumin
CA	Cryoablation
DMSO	dimethyl sulfoxide
ELISA	enzyme-linked immunosorbent assay
HGF	hepatocyte growth factor
HPF	high-power field
IACUC	institutional animal care and use committee
IHC	immunohistochemistry
PEG	polyethylene glycol
PFD	pirfenidone

References

[1]. Blobe GC, Schiemann WP, Lodish HF, Role of transforming growth factor beta in human disease, The New England journal of medicine, 342 (2000) 1350–1358. [PubMed: 10793168]

[2]. Chen JF, Ni HF, Pan MM, Liu H, Xu M, Zhang MH, Liu BC, Pirfenidone inhibits macrophage infiltration in 5/6 nephrectomized rats, American journal of physiology. Renal physiology, 304 (2013) F676–685. [PubMed: 23152296]

[3]. Choi SH, Nam JK, Jang J, Lee HJ, Lee YJ, Pirfenidone enhances the efficacy of combined radiation and sunitinib therapy, Biochemical and biophysical research communications, 462 (2015) 138–143. [PubMed: 25935484]

[4]. Chung SW, Kwon MY, Kang YH, Chung HT, Lee SJ, Kim HP, Perrella MA, Transforming growth factor-beta1 suppression of endotoxin-induced heme oxygenase-1 in macrophages involves activation of Smad2 and downregulation of Ets-2, J Cell Physiol, 227 (2012) 351–360. [PubMed: 21437904]

[5]. Cressman DE, Diamond RH, Taub R, Rapid activation of the Stat3 transcription complex in liver regeneration, Hepatology (Baltimore, Md.), 21 (1995) 1443–1449.

[6]. Erinjeri JP, Thomas CT, Samoilia A, Fleisher M, Gonen M, Sofocleous CT, Thornton RH, Siegelbaum RH, Covey AM, Brody LA, Alago W Jr., Maybody M, Brown KT, Getrajdman GI, Solomon SB, Image-guided thermal ablation of tumors increases the plasma level of interleukin-6 and interleukin-10, J Vasc Interv Radiol, 24 (2013) 1105–1112. [PubMed: 23582441]

[7]. European Medicines Agency, Esbriet 267 mg hard capsules (PDF), Summary of product characteristics.

[8]. Ferrari G, Cook BD, Terushkin V, Pintucci G, Mignatti P, Transforming growth factor-beta 1 (TGF-beta1) induces angiogenesis through vascular endothelial growth factor (VEGF)-mediated apoptosis, J Cell Physiol, 219 (2009) 449–458. [PubMed: 19180561]

[9]. Gazzaniga S, Bravo A, Goldszmid SR, Maschi F, Martinelli J, Mordoh J, Wainstok R, Inflammatory changes after cryosurgery-induced necrosis in human melanoma xenografted in nude mice, J Invest Dermatol, 116 (2001) 664–671. [PubMed: 11348453]

[10]. Gilbert KM, Thoman M, Bauche K, Pham T, Weigle WO, Transforming growth factor-beta 1 induces antigen-specific unresponsiveness in naive T cells, Immunological investigations, 26 (1997) 459–472. [PubMed: 9246566]

[11]. Grivennikov S, Karin E, Terzic J, Mucida D, Yu GY, Vallabhapurapu S, Scheller J, Rose-John S, Cheroutre H, Eckmann L, Karin M, IL-6 and Stat3 are required for survival of intestinal epithelial cells and development of colitis-associated cancer, Cancer cell, 15 (2009) 103–113. [PubMed: 19185845]

[12]. Grivennikov SI, Greten FR, Karin M, Immunity, inflammation, and cancer, Cell, 140 (2010) 883–899. [PubMed: 20303878]

[13]. Hsia CY, Huo TI, Chiang SY, Lu MF, Sun CL, Wu JC, Lee PC, Chi CW, Lui WY, Lee SD, Evaluation of interleukin-6, interleukin-10 and human hepatocyte growth factor as tumor markers for hepatocellular carcinoma, European journal of surgical oncology : the journal of the European Society of Surgical Oncology and the British Association of Surgical Oncology, 33 (2007) 208–212.

[14]. Jang JW, Oh BS, Kwon JH, You CR, Chung KW, Kay CS, Jung HS, Serum interleukin-6 and C-reactive protein as a prognostic indicator in hepatocellular carcinoma, Cytokine, 60 (2012) 686–693. [PubMed: 22906998]

[15]. Jiang J, Goel R, Schmechel S, Vercellotti G, Forster C, Bischof J, Pre-conditioning cryosurgery: cellular and molecular mechanisms and dynamics of TNF-alpha enhanced cryotherapy in an in vivo prostate cancer model system, Cryobiology, 61 (2010) 280–288. [PubMed: 20940007]

[16]. Kim ES, Keating GM, Pirfenidone: a review of its use in idiopathic pulmonary fibrosis, Drugs, 75 (2015) 219–230. [PubMed: 25604027]

[17]. Li MO, Wan YY, Sanjabi S, Robertson AK, Flavell RA, Transforming growth factor-beta regulation of immune responses, Annual review of immunology, 24 (2006) 99–146.

[18]. Matzinger P, The danger model: a renewed sense of self, Science, 296 (2002) 301–305. [PubMed: 11951032]

[19]. Rozenblum N, Zeira E, Bulvik B, Gourevitch S, Yotvat H, Galun E, Goldberg SN, Radiofrequency Ablation: Inflammatory Changes in the Periablative Zone Can Induce Global Organ Effects, including Liver Regeneration, Radiology, 276 (2015) 416–425. [PubMed: 25822472]

[20]. Sabel MS, Cryo-immunology: a review of the literature and proposed mechanisms for stimulatory versus suppressive immune responses, Cryobiology, 58 (2009) 1–11. [PubMed: 19007768]

[21]. Sabel MS, Su G, Griffith KA, Chang AE, Rate of freeze alters the immunologic response after cryoablation of breast cancer, Ann Surg Oncol, 17 (2010) 1187–1193. [PubMed: 20033323]

[22]. Sakaguchi S, Yamaguchi T, Nomura T, Ono M, Regulatory T cells and immune tolerance, Cell, 133 (2008) 775–787. [PubMed: 18510923]

[23]. Schneider CA, Rasband WS, Eliceiri KW, NIH Image to ImageJ: 25 years of image analysis, Nature methods, 9 (2012) 671–675. [PubMed: 22930834]

[24]. Shihab FS, Bennett WM, Yi H, Andoh TF, Pirfenidone treatment decreases transforming growth factor-beta1 and matrix proteins and ameliorates fibrosis in chronic cyclosporine nephrotoxicity, American journal of transplantation : official journal of the American Society of Transplantation and the American Society of Transplant Surgeons, 2 (2002) 111–119.

[25]. Spagnolo P, Sverzellati N, Rossi G, Cavazza A, Tzouvelekis A, Crestani B, Vancheri C, Idiopathic pulmonary fibrosis: an update, Annals of medicine, 47 (2015) 15–27. [PubMed: 25613170]

[26]. Tiemessen MM, Kunzmann S, Schmidt-Weber CB, Garssen J, Bruijnzeel-Koomen CA, Knol EF, van Hoffen E, Transforming growth factor-beta inhibits human antigen-specific CD4+ T cell proliferation without modulating the cytokine response, International immunology, 15 (2003) 1495–1504. [PubMed: 14645158]

[27]. Togami K, Miyao A, Miyakoshi K, Kanehira Y, Tada H, Chono S, Efficient delivery to human lung fibroblasts (WI-38) of pirfenidone incorporated into liposomes modified with truncated basic fibroblast growth factor and its inhibitory effect on collagen synthesis in idiopathic pulmonary fibrosis, Biological & pharmaceutical bulletin, 38 (2015) 270–276. [PubMed: 25747986]

[28]. Wahl SM, Hunt DA, Wong HL, Dougherty S, McCartney-Francis N, Wahl LM, Ellingsworth L, Schmidt JA, Hall G, Roberts AB, et al., Transforming growth factor-beta is a potent

immunosuppressive agent that inhibits IL-1-dependent lymphocyte proliferation, Journal of immunology (Baltimore, Md. : 1950), 140 (1988) 3026–3032.

[29]. Wahl SM, Wen J, Moutsopoulos N, TGF-beta: a mobile purveyor of immune privilege, Immunological reviews, 213 (2006) 213–227. [PubMed: 16972906]

[30]. Wong VW, Yu J, Cheng AS, Wong GL, Chan HY, Chu ES, Ng EK, Chan FK, Sung JJ, Chan HL, High serum interleukin-6 level predicts future hepatocellular carcinoma development in patients with chronic hepatitis B, Int J Cancer, 124 (2009) 2766–2770. [PubMed: 19267406]

[31]. Yao Z, Fenoglio S, Gao DC, Camiolo M, Stiles B, Lindsted T, Schlederer M, Johns C, Altorki N, Mittal V, Kenner L, Sordella R, TGF-beta IL-6 axis mediates selective and adaptive mechanisms of resistance to molecular targeted therapy in lung cancer, Proc Natl Acad Sci U S A, 107 (2010) 15535–15540. [PubMed: 20713723]

[32]. Zhou YH, Liao SJ, Li D, Luo J, Wei JJ, Yan B, Sun R, Shu Y, Wang Q, Zhang GM, Feng ZH, TLR4 ligand/H(2)O(2) enhances TGF-beta1 signaling to induce metastatic potential of non-invasive breast cancer cells by activating non-Smad pathways, PLoS One, 8 (2013) e65906. [PubMed: 23734265]

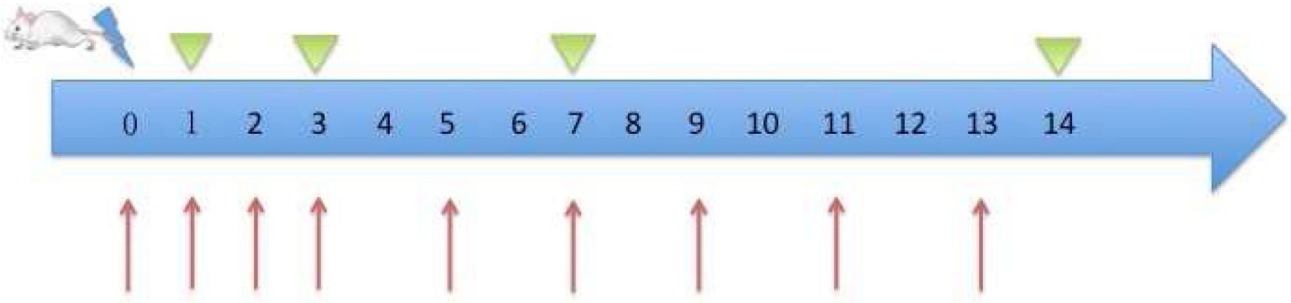

Fig 1. Study protocol

80 mice were randomly divided into four groups: 1) sham + vehicle, 2) sham + PFD, 3) CA + vehicle, and 4) CA + PFD

cryoablation

blood and tissue sample collection

PFD intraperitoneal injection or vehicle injection

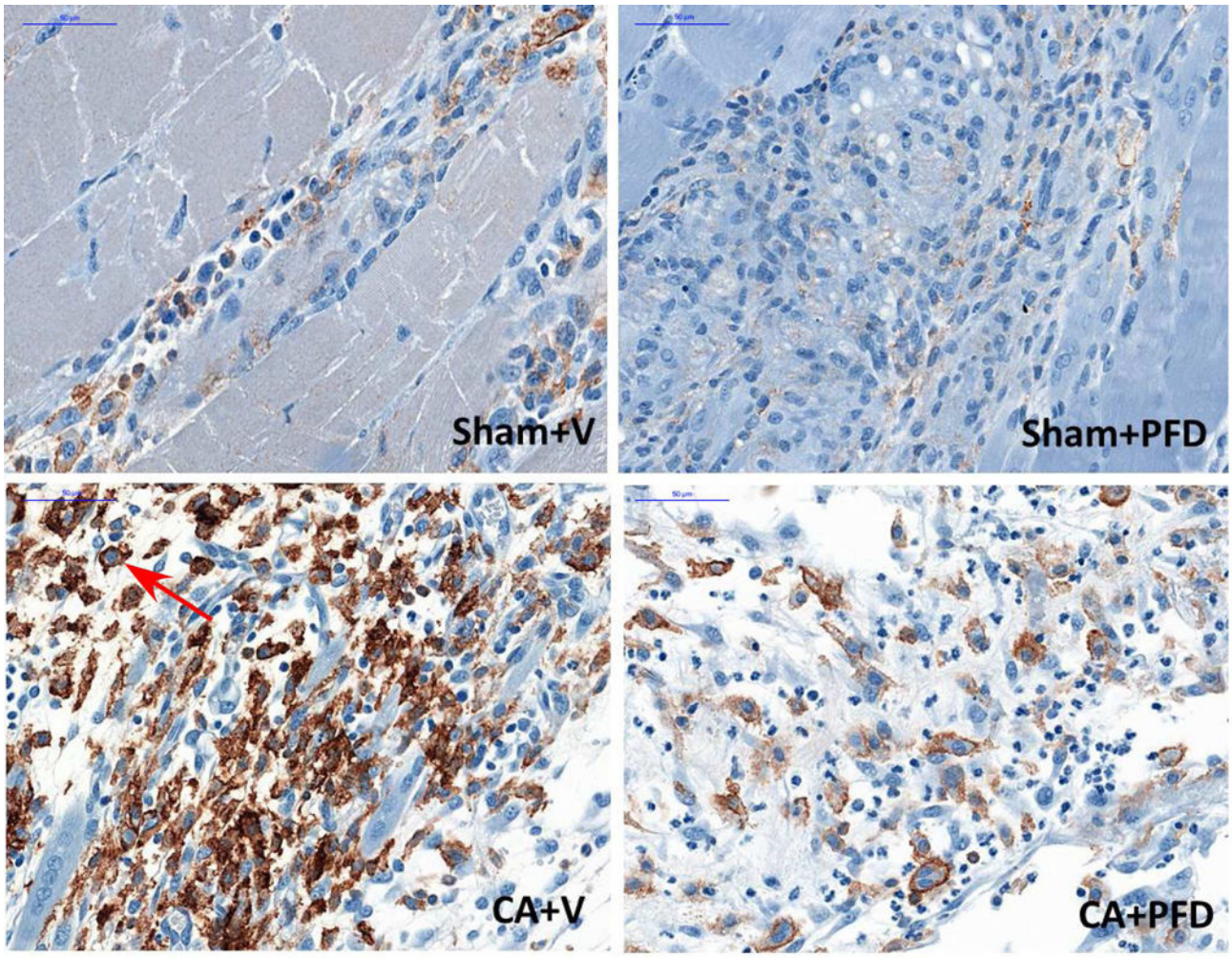

Fig 2a.

F4/80 staining (original magnification, ×40) shows macrophage accumulation at border zone 7 days after cryoablation in different groups (five mice per group, scale bar = 200 μm). Marked macrophage accumulation (arrow) is noted.

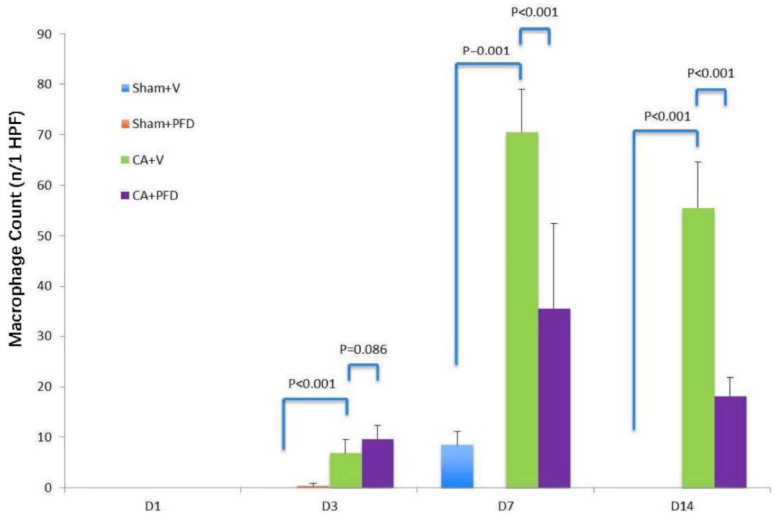

Fig 2b.

Bar chart shows quantification of macrophages at the border zone. Macrophages peaked at 7 days after cryoablation. PFD decreased cryoablation-induced macrophage infiltration ($p<0.001$).

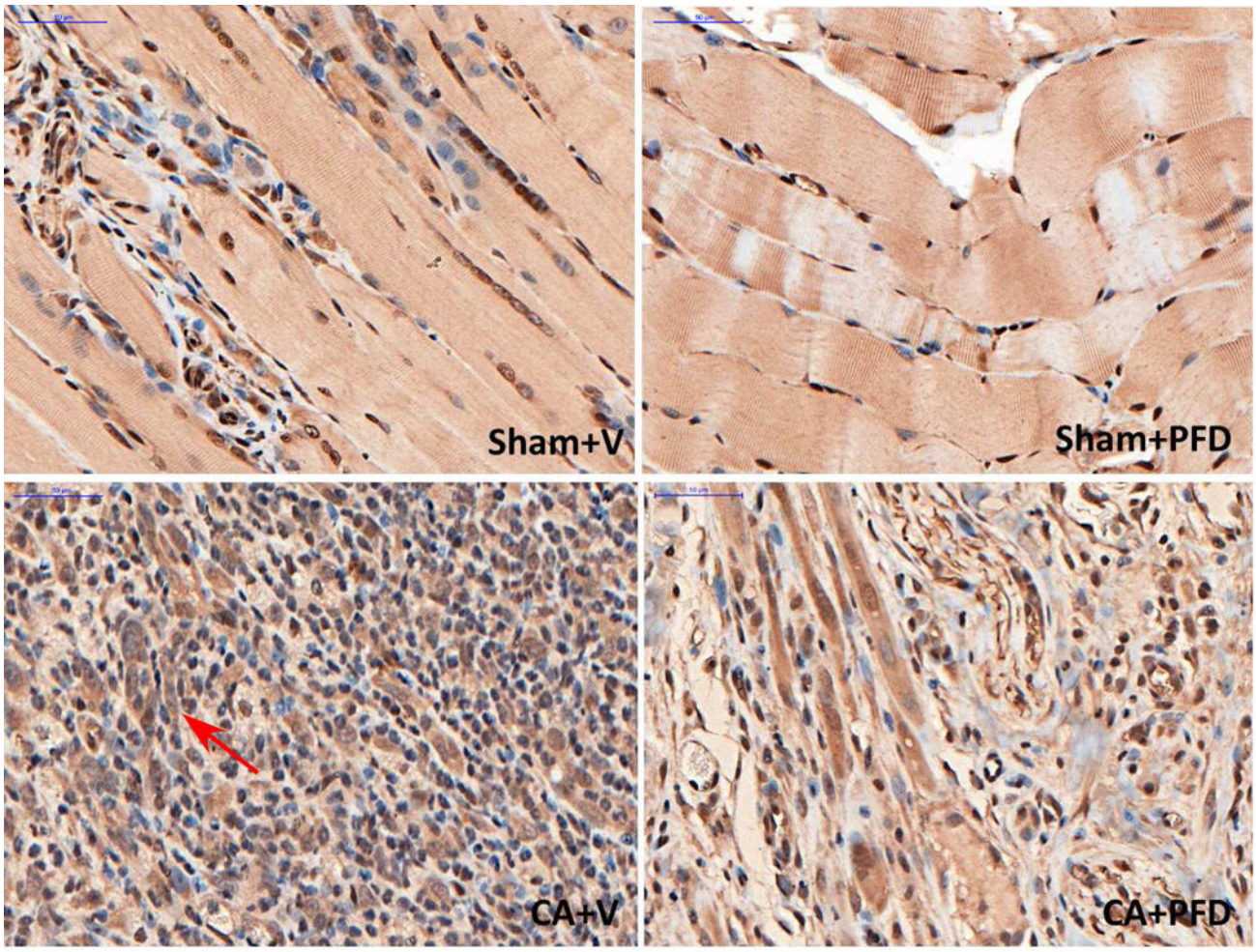

Fig 3a.

TGFβ1 staining (original magnification, ×40) shows TGFβ1 expression at the border zone 14 days after cryoablation in different groups (five mice per group, scale bar = 200 μm). Marked local TGFb1 staining (arrow) is noted.

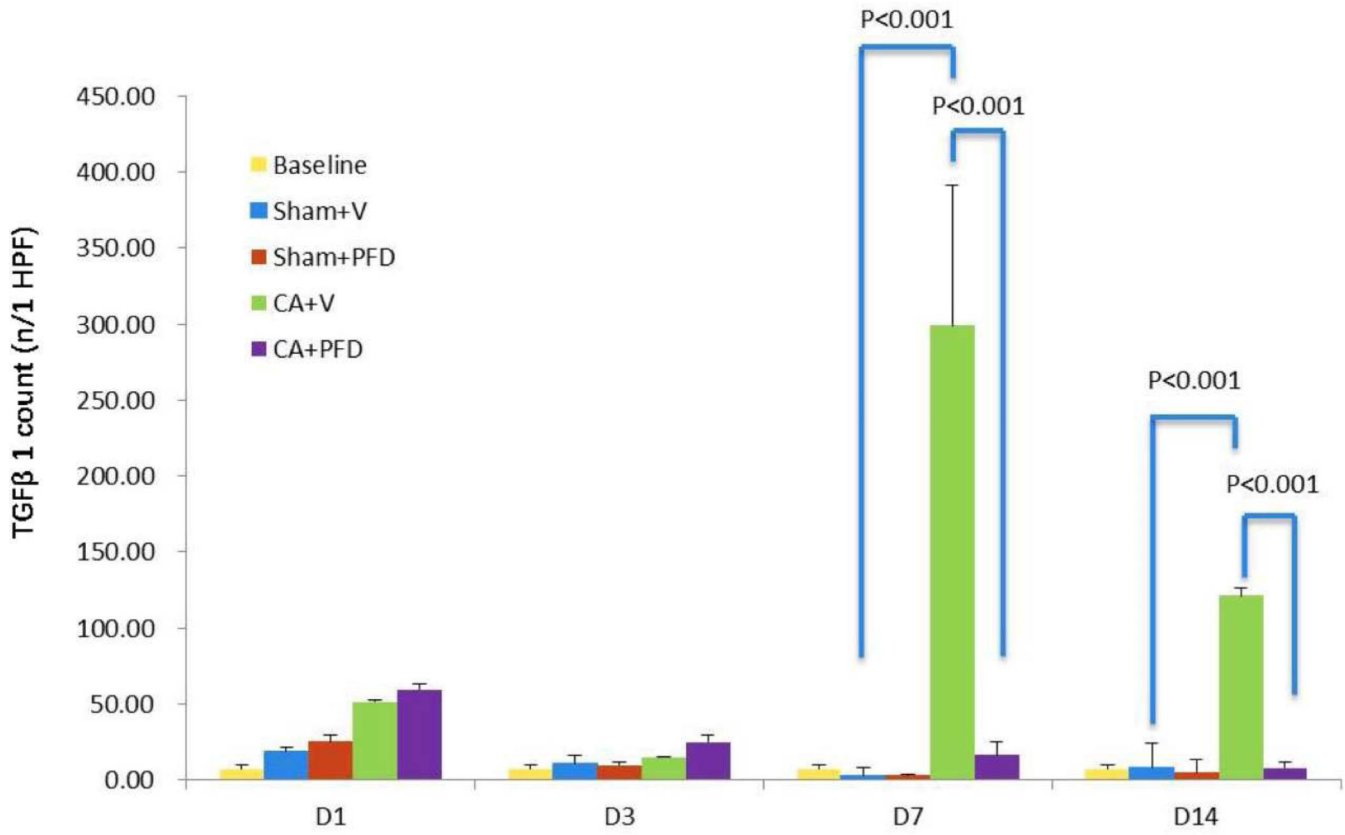

Fig 3b.

Bar chart shows quantification of TGFβ1 expression at the border zone. TGFβ1 expression peaks at 14 days after cryoablation. PFD decreases cryoablation-induced TGFβ1 expression ($p<0.001$).

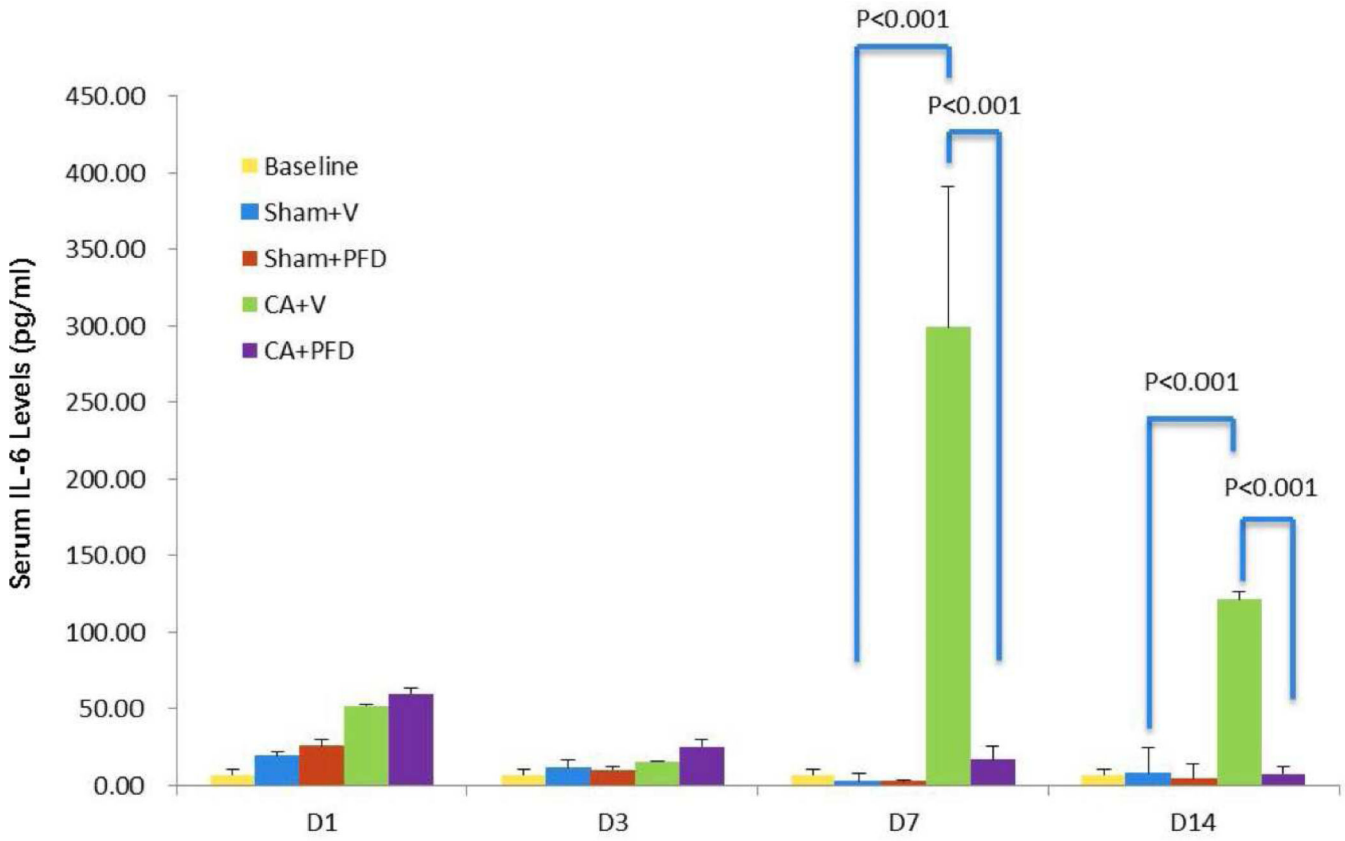

Fig 4.

Bar chart shows serum IL-6 levels at different timepoints after cryoablation. IL-6 level peaks at 7 days after cryoablation. PFD decreases cryoablation-induced serum IL-6 level elevation ($p<0.001$).

Table 1

Post-CA macrophage infiltration in a geographic rim surrounding the CA zoneat different time points

Timepoint	Sham+V	Sham+PFD	CA+V	CA+PFD
D1	0±0	0±0	0±0	0±0
D3	0±0	0.33±0.52	6.86±2.61	9.57±2.82
D7	8.5±2.59	0±0	70.5±8.46	35.5±16.93
D14	0±0	0±0	55.5±9.07	18.2±3.66

Note: D=day, V=vehnicle, PFD=pirfenidone, CA=cryoablation

Table 2

Post-CA local TGFβ1 expression in a geographic rim surrounding the CA zone at different time points

Timepoint	Sham+V	Sham+PFD	CA+V	CA+PFD
D1	11.8±2.77	10.2±2.39	36.8±5.02	33.6±2.51
D3	14.6±4.56	13±4.3	104.2±16.3	92±12.66
D7	34±9.67	3±0.71	183±9.59	60.2±7.6
D14	41.4±4.61	5.4±1.82	228±18.36	65.6±8.73

Note: D=day, V=vehicle, PFD=pirfenidone, CA=cryoablation

Table 3

Post-CA serum cytokine levels at different time points

Cytokine (pg/ml)	Baseline (pg/ml)	Time point	Group			
			Sham+V	Sham+PFD	CA+V	CA+PFD
IL-6	7.33±2.09	D1	18.33±2.66	25.15±6.01	51.25±5.09	59.38±15.85
		D3	10.41±3.9	9.62±1.99	14.9±0.6	24.9±8.55
		D7	2.71±1.08	3.04±0.03	298.67±92.63 *,#	16.28±4.76
		D14	7.93±4.22	4.91±4.13	121.33±8.62 *,#	7.78±3.84
IL-10	9.56±1.04	D1	9.4±1.74	5.74±0.52	6.74±0.94	8.53±2
		D3	6.62±1.2	8.82±1.98	8.13±2.18	9.19±1.72
		D7	8.46±1.63	6.82±0.33	9.96±1.43	9.06±1.07
		D14	6.7±2.13	11.24±1.85	12.04±3.75	9.5±1.23
TGFβ1	11020.86±6982.82	D1	15013.69±8676.46	10879.05±4768.49	11746.09±4059.83	6976.26±1503.01
		D3	8141.17±2988.41	5694.94±602.08	9741.66±2867.82	5823.13±481.15
		D7	6807.76±1109.73	7095.07±1355.21	7822.44±2453.08	10447.42±3252.91
		D14	4048.39±242.97	4344.87±1012.34	13196.18±14347.3	8497.5±10993.84

Note: D=day, V=vehicle, PFD=pirfenidone, CA=cryoablation

* p<0.001 compared to Sham + Vehicle group

# p<0.001 compared to CA + PFD group